RSC Advances

ROYAL SOCIETY OF CHEMISTRY

www.rsc.org/advances

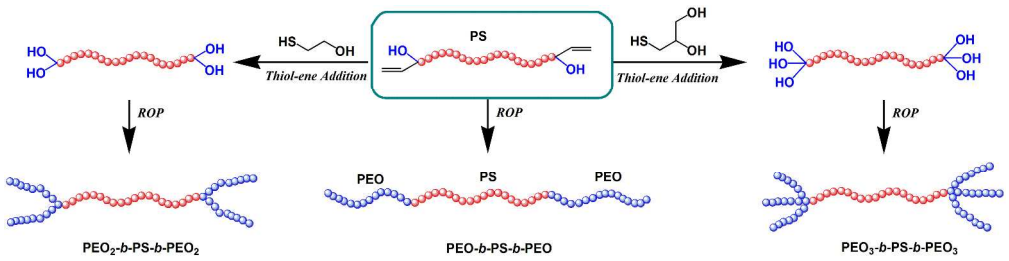

Series of well-defined dumbbell-shaped copolymers PEOx-b-PS-b-PEOx (x=1, 2, 3) consisting of PEO and PS segments were successfully synthesized by LAP, ROP mechanism and the efficient thiol-ene addition reaction. This versatile synthetic route might be further explored to synthesize other copolymers with complicated architectures and defined molecular weights.
431x108mm (300 x 300 DPI)

Cite this: DOI: 10.1039/c0xx00000x

www.rsc.org/xxxxxx

ARTICLE TYPE

Synthesis and Characterization of Novel Dumbbell-shaped Copolymers of Poly(ethylene oxide)$_x$-*b*-polystyrene-*b*-poly(ethylene oxide)$_x$ with Tunable Side Arms by Combination of Efficient Thiol-ene Coupling Reaction with Living Anionic Polymerization Mechanism

Lingdi Chen, Jian Huang, Xuepu Wang, Chengjiao Lu, Hongdong Zhang* and Guowei Wang*

Received (in XXX, XXX) Xth XXXXXXXXX 20XX, Accepted Xth XXXXXXXXX 20XX
DOI: 10.1039/b000000x

Series of novel dumbbell-shaped copolymers poly(ethylene oxide)$_x$-*b*-polystyrene-*b*-poly(ethylene oxide)$_x$ (PEO$_x$-*b*-PS-*b*-PEO$_x$, x=1, 2, 3) composed of different numbers of hydrophilic PEO and hydrophobic PS segments were prepared by combination of living anionic polymerization (LAP) with ring opening polymerization (ROP) mechanisms, and the efficient thiol-ene addition reaction was also adopted. First, the functional polystyrene with one hydroxyl group and one allyl group at each end (AGE-PS-AGE) was synthesized by LAP of St monomers and the following capping reaction with allyl glycidyl ether (AGE). Subsequently, by thiol-ene addition reaction with 2-mercaptoethanol (ME) and 3-mercapto-1,2-propanediol (MP), one allyl group on AGE-PS-AGE were transferred into one or two hydroxyl groups to synthesize the functional polystyrene with two hydroxyl groups at both end (ME-PS-ME) and three hydroxyl groups at both end (MP-PS-MP). Then, the copolymers PEO$_x$-*b*-PS-*b*-PEO$_x$ were achieved by ROP of EO monomers using AGE-PS-AGE, ME-PS-ME and MP-PS-MP as macro-initiators, respectively. The target copolymers and their precursors were well characterized by GPC, ^{1}H NMR and ^{13}C NMR measurements. The crystallization behavior of copolymers with different topologies and compositions were investigated by DSC, XRD and POM instruments, respectively, and the results showed that the topologies tend to give primary contribution than the compositions did.

Introduction

In recent years, with the rapid development of living / controlled polymerization mechanisms and efficient coupling methods, a variety of polymers with complicated architectures and compositions had be realized by certain synthetic route.[1] The unique architectures included the graft,[2] hyper-branched,[3] cyclic,[4] dendritic,[5] star-shaped,[6] and so on,[7] and the compositions could be covered by plenty of segments derived from any polymerizable monomers. All these achievements could be attributed to the increasing attention on their unique physical properties in solution and bulk, as well as their versatile applications, including biomedical materials,[8] nanotechnology,[9] composite materials[10] and supra-molecular science.[11]

Among all the compositions, the polystyrene (PS) is a typical hydrophobic and amorphous segment, and poly(ethylene oxide) (PEO) is a hydrophilic and crystalline segment. Because of these characteristics, the copolymers contained both PS and PEO segments have been widely studied and utilized for various applications. For example, the common models were the copolymers of PS-*b*-PEO, PS-*b*-PEO-*b*-PS or PEO-*b*-PS-*b*-PEO with the simplest topologies. The research priorities on these copolymers were focused on the microphase separated morphology, [12] thermodynamic properties, [13] crystallization behavior, [14] and aggregate morphologies. [15] As for their applications, these copolymers could be served as template for porous materials[16] and micro / nanopatterns[17] based on their interesting self-assembly morphologies.[18] However, up to now, the copolymers composed by PEO and PS segments with complicated architectures and defined molecular weight are still rarely researched, which might be attributed to the somewhat difficult synthesis procedure of these copolymers.

For the copolymers with complicated architectures, the mere polymerization mechanism usually could not reach the target. Additionally, some efficient coupling reactions would also play an important role in the synthesis of these copolymers. Till recently, the innovatively presented coupling reactions with "click" character included the Thiol-bromide reaction,[19] Thiol-ene addition,[20] Thiol-yne addition,[21] Atom Transfer Radical Coupling (ATRC) reaction,[22] Glaser coupling,[23] Suzuki reaction,[24] Copper Catalyzed Azide / Alkyne Click (CuAAC) Chemistry and Diels-Alder (DA) [4+2] reaction,[1f] and so on. Because of their high efficiencies and particular versatility, these reactions were widely used in polymer chemistry. Among these coupling reactions, the Thiol-ene addition reaction has been widely adopted because of its high efficiency and tolerance to water and functional groups, as well as its easy operation under the photochemical initiation. The concerned applications included nanotechnology,[25] composites,[26] biochemistry,[27] and adhesives.[28] Correspondingly, various monomers contained vinyl and thiol

groups were designed and their Thiol-ene addition reactions were well researched. [29] For example, Hawker, [30] Son [31] and Malmstrom [32] had synthesized several dendrimers via this versatile Thiol-ene addition reaction. Hawker, [33] Kornfield, [34] Schlaad [35] and Sengupta [36] prepared several functionalized polymers (such as PS, poly(butadiene) (PB), and poly(propylene) (PP)) by using this technique under feasible and mild conditions, as well as the telechelic polymers were also realized by Sumerlin[37] and Maynard.[38] Thus, this thiol-ene "click" chemistry had been actually proved to be an efficient, robust and orthogonal tool in polymer chemistry.

In this contribution, considered the above limitation on copolymers composed by PEO and PS segments with different architectures and defined molecular weights, we aim to synthesize some novel dumbbell-shaped copolymers of PEO_x-*b*-PS-*b*-PEO_x (x=1, 2, 3) with tunable side arms (Scheme 1). The PS segment with controlled molecular weight could be realized by typical living anionic polymerization (LAP) mechanism, and the PEO segment could be synthesized by ring opening polymerization (ROP) mechanism. Also, the Thiol-ene "click" chemistry was adopted to modify the functionalized intermediate to tune the initiating sites (corresponding to the tunable arms of target copolymers) on macro-initiators. On the other hand, in previous work, some researchers had studied the crystallization behavior of copolymers composed by PEO and PS segments.[39] These works were all focused on the effect of compositions on their crystallization behavior, and the topologies were less considered.[40] Thus, in this contribution, as another important task, the crystallization behavior of the synthesized copolymers with close compositions but different topologies are also investigated and compared.

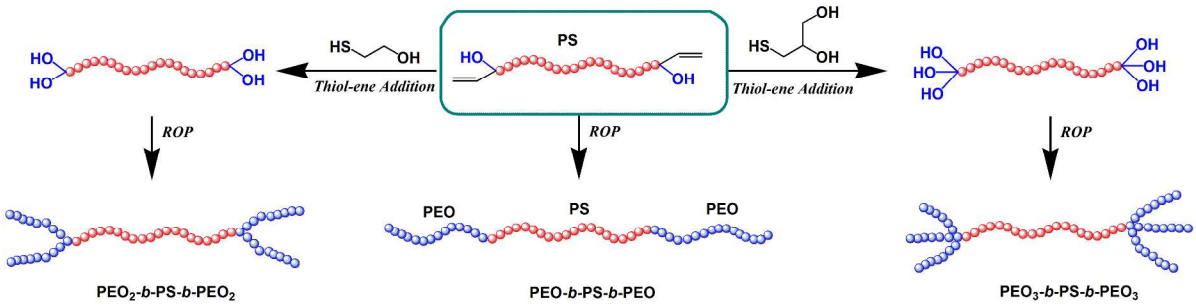

Scheme 1. The illustration of synthetic procedure of copolymers PEO_x-*b*-PS-*b*-PEO_x.

Experimental

Materials

Styrene [St, 99%, Sinopharm Chemical Reagent Co. (SCR)] was washed with 10% NaOH aqueous solution followed by water three times successively, dried over anhydrous $MgSO_4$ for 24 h, further dried over CaH_2 and distilled under reduced pressure before use. Allyl glycidyl ether (AGE, Aldrich, 99 %) was dried over CaH_2 and distilled under reduced pressure before use. Ethylene oxide (EO, SCR, 99 %) was dried over CaH_2 and distilled before use. Naphthalene (SCR, AR) was purified by sublimation. Tetrahydrofuran (THF, SCR, 99 %) was refluxed and distilled from potassium naphthalenide solution. Azobisisobutyronitrile (AIBN, SCR, 99 %), *n*-butyllithium (*n*-BuLi, 1.6 M solution in hexanes, J&K), 2-mercaptoethanol (ME, Aldrich, 98 %), 3-mercapto-1,2-propanediol (MP, Aldrich, 98 %) were used as received. Diphenylmethyl potassium (DPMK) with concentration of 0.75 mol/L was prepared as described elsewhere.[15b] All other reagents and solvents were purchased from SCR and used as received except for declaration.

Characterization

Gel permeation chromatographic (GPC) of polymers was performed in THF at 35 °C with an elution rate of 1.0 mL/min on an Agilent 1100 equipped with a G1310A pump, a G1362A refractive index detector, and a G1314A variable wavelength detector. One 5-μm LP gel column (500 Å, molecular range 500-2×10^4 g/mol) and two 5 μm LP gel mixed bed column (molecular range 200-3×10^6 g/mol) were calibrated by PS standards. ^{1}H NMR spectra were recorded on a Bruker (400 MHz) spectrometer in $CDCl_3$ with tetramethylsilane (TMS) as the internal standard. The MALDI-TOF MS measurement was performed using a Perspective Biosystem Voyager-DE STR MALDI-TOF(matrix-assisted laser desorption/ionization time-of-flight) mass spectrometer (PE Applied Biosystems, Framingham, MA). Accelerating voltage, grid voltage and delay time were optimized for each sample and all the spectra were recorded in reflectron mode. Matrix solution of dithranol (20mg/ml), end-functionalized polymer (10mg/ml) and cationizing salt of silver trifluoroacetate (10mg/ml) in THF were mixed in the ratio of matrix: cationizing salt: polymer =10:1:2, and 0.8μL of mixed solution was deposited on the sample holder (well-plate). Differential scanning calorimetry (DSC) was carried on a DSC Q2000 thermal analysis system (Shimadzu, Japan). The samples were first heated from -80 °C to 150 °C at a heating rate of 10°C /min under nitrogen atmosphere, followed by cooled to -80 °C at 10 °C /min after stopping at 150°C for 5 min, and finally heated to 150 °C at 10 °C /min after stopping at -80 °C for 5 min. X-ray diffraction (XRD) measurements were carried out using an XPert PRO (PANalytical) with Cu Kα (1.541 Å) radiation (40 kV, 40 mA). Samples were exposed at a scanning rate of 2θ=5 °C/min between 2θ values of 10° to 40°. Crystal growth was observed under a

polarized optical microscope (POM, Leica, DM 2500P). The concentration of copolymer was 5mg/mL and dichloromethane (CH_2Cl_2) was used as solvent, and all the measurements were carried out at 25 °C.

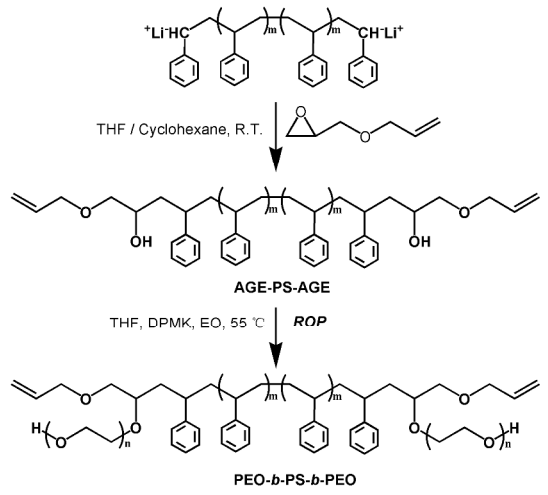

Scheme 2. The synthetic procedure of copolymers PEO-*b*-PS-*b*-PEO and its precursor.

Synthesis of Polystyrene Functionalized with Allyl Glycidyl Ether (AGE-PS-AGE)

The sample of AGE-PS-AGE was obtained by LAP of St monomers initiated by lithium naphthalenide and the following end-capping reaction with AGE agent (Scheme 2). The initiator of lithium naphthalenide was first synthesized from naphthalene and lithium according to our previous work, [41] and the concentration of 0.71 mol/L was analyzed by titration using hydrochloric acid (0.1 mol/L). Typically, cyclohexane (700 mL), styrene (50.0 mL, 0.43 mol), and THF (6.0 mL) were sequentially introduced into a 1 L ampule. In order to consume the remained impurities in ampule, *n*-Bu^-Li^+ solution was firstly added dropwise till the mixture turned yellowish, and then the needed lithium naphthalenide solution (35.0 mL, 24.9 mmol) was added rapidly. After the reaction was stirred at 25 °C for 50 min, the AGE agent (10.0 mL, 84.5 mmol) dissolved in THF (20 mL) was added, and the red solution changed into faint yellow immediately. The solution was stirred for another 2.0 h at 25 °C and terminated with acidic methanol (0.1 HCl in CH_3OH). After all the solvents were evaporated, the product was recovered by thrice precipitation in methanol and dried under vacuum at 45 °C. Yield: 44.6 g (98 %) ^{1}H NMR ($CDCl_3$) δ (ppm): 1.11-2.25 ($C_6H_5CHCH_2$-), 2.98-3.30 (-CH_2CHOH), 3.56-3.48 (-CH_2CHOH), 3.74-3.80 (-CH_2OCH_2-), 5.08-5.25 (CH_2=CH-), 5.74-5.86 (CH_2=CH-), 6.28-7.22 (-C_6H_5-). $M_{n,GPC}$=3,700 g/mol, PDI=1.10, $M_{MALDI\text{-}TOF\ MS}$=2,500 g/mol.

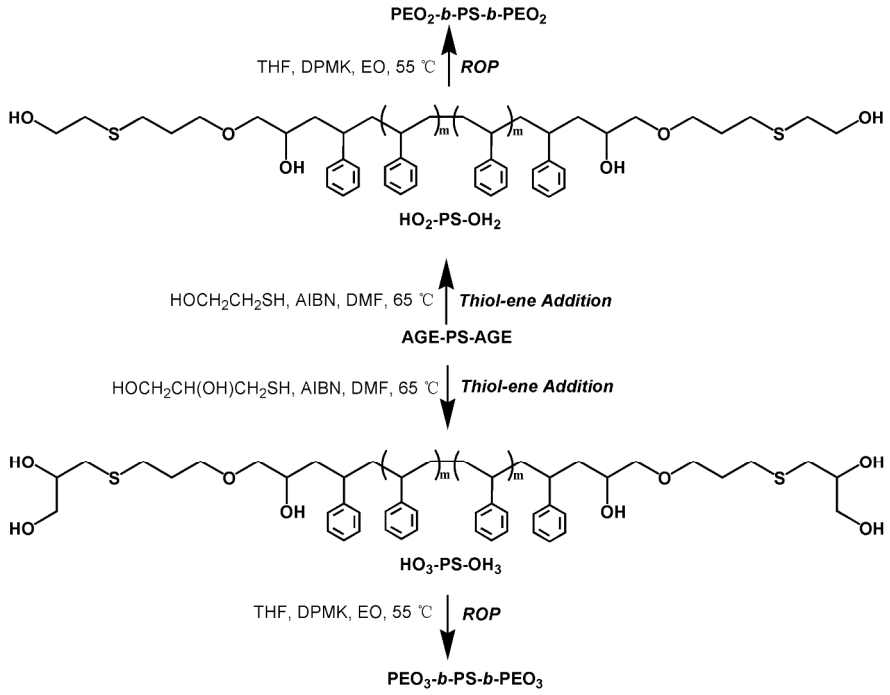

Scheme 3. The synthetic procedure of copolymers PEO_2-*b*-PS-*b*-PEO_2, PEO_3-*b*-PS-*b*-PEO_3 and their precursor.

Synthesis of Polystyrene Functionalized with 2-Mercaptoethanol and 3-Mercapto-1, 2-propanediol (ME-PS-ME and MP-PS-MP)

The functionalized precursors of ME-PS-ME and MP-PS-MP were achieved by thiol-ene addition reaction (Scheme 3). Typically, AGE-PS-AGE (10.0 g, 2.7 mmol), AIBN (1.64 g, 10 mmol) and ME (2.5 mL, 25 mmol) were dissolved in 80.0 mL dimethylformamide (DMF) in a 200 mL ampoule. After the reaction system was degassed by three cycles of freeze−pump−thaw, the ampoule was filled with nitrogen and then maintained at 65 °C for 24 h. Finally, the solvents were removed by reduced distillation, and the ME-PS-ME was obtained by thrice precipitation in methanol and dried under

vacuum at 45 °C. Yield: 9.8 g (96 %). ^{1}H NMR ($CDCl_3$) δ (ppm): 1.20-2.10 ($C_6H_5CHCH_2$-), 2.45-2.69 (-CH_2SCH_2-), 2.98-3.14 (-CH_2OH), 3.69-3.78 (-CH_2OCH_2-), 2.32-3.49 (-CHOH), 6.33-7.25 (-C_6H_5-).

Similarly, the synthetic procedure of MP-PS-MP was the same as that of ME-PS-ME, except that the ME agent was replaced by MP agent. ^{1}H NMR ($CDCl_3$) δ (ppm):1.16-2.20 ($C_6H_5CHCH_2$-), 2.52-2.72 (-CH_2SCH_2-), 2.92-3.15 (-CH_2OH), 3.34-3.59 (-CHOH), 3.61-3.83 (-CH_2OCH_2-), 6.24-7.28 (-C_6H_5-).

Synthesis of Dumbbell-shaped Copolymer PEO_x-*b*-PS-*b*-PEO_x (x=1, 2, 3)

The copolymer PEO-*b*-PS-*b*-PEO was obtained by ROP of EO monomers using AGE-PS-AGE as macro-initiator (Scheme 3). Typically, the dry AGE-PS-AGE (6.0 g, 1.6 mmol) was dissolved in 200 mL THF and charged into a 500 mL dry ampoule, and the calculated DPMK solution (4.0 mL, 3.0 mmol) was added dropwisely by a syringe under magnetic stirring. Then the ampoule was placed into an ice bath and cold EO (15.0 mL, 0.29 mol) monomers were added quickly, and the solution was heated to 55 °C and stirred for 96 h. The solution was finally terminated by acid methanol (0.1 HCl in CH_3OH) and the solvents were evaporated. Subsequently, the copolymers PEO-*b*-PS-*b*-PEO were precipitated into cold petroleum ether (30-60 °C) slowly for three times and dried under vacuum at 45 °C for 12 h till to a constant weight Yield: 9.8 g (96 %). ^{1}H NMR ($CDCl_3$) δ (ppm): 3.59-3.61 (-CH_2CH_2O-), 6.33-7.25 (-C_6H_5-). $M_{n,GPC}$=11,500 g/mol, PDI=1.10, $M_{n,NMR}$=11,000 g/mol.

Similarly, the copolymers of PEO_2-*b*-PS-*b*-PEO_2 and PEO_3-*b*-PS-*b*-PEO_3 were also prepared by ROP of EO monomers from macro-initiators of ME-PS-ME and MP-PS-MP, respectively (Scheme 3). By changing the feed molar ratio of macro-initiators to EO monomers, the copolymers with different compositions could be realized.

Results and Discussion

Synthesis and Characterization of Amphiphilic Dumbbell-shaped Copolymers of PEO_x-*b*-PS-*b*-PEO_x

The key precursor AGE-PS-AGE with one active hydroxyl group and one allyl group at each end was designed and synthesized by LAP mechanism and the subsequent end-capping reaction with oxirane ring on AGE. This versatile precursor could be further selectively modified by thiol-ene addition reaction. Subsequently, by combination of ROP mechanism, the target copolymer PEO_x-*b*-PS-*b*-PEO_x (x=1, 2, 3) with different numbers of arms and compositions could be conveniently realized.

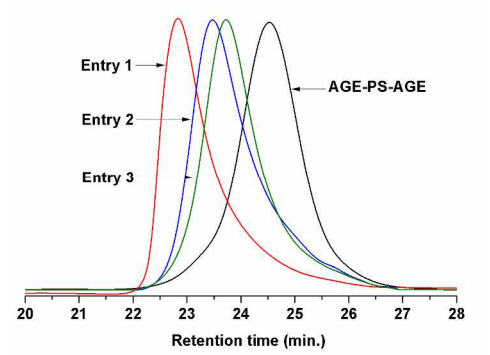

Fig. 1 GPC traces of polymers AGE-PS-AGE (M_n=3,700 g/mol, PDI=1.10), PEO-*b*-PS-*b*-PEO (Entry 1, M_n=11,500 g/mol, PDI= 1.11), PEO_2-*b*-PS-*b*-PEO_2 (Entry 2, M_n=7,700 g/mol, PDI= 1.16), PEO_3-*b*-PS-*b*-PEO_3 (Entry 3, M_n=7,600 g/mol, PDI=1.10).

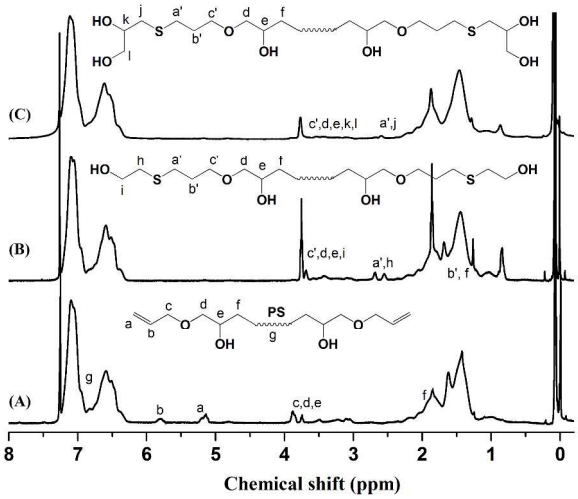

Fig. 2 ^{1}H NMR spectra of (A) AGE-PS-AGE, (B) ME-PS-ME, and (C) MP-PS-MP (in $CDCl_3$).

Firstly, the difunctional living $^+$Li-PS$^-$Li$^+$ species grew from lithium naphthalenide were carefully end-capped with AGE agent. According to previous work by Quirk,[42] they had synthesized several functionalized polymers with high efficiencies (usually > 95.0 %) by capping the living species with oxirane ring on substituted epoxy, such as 1-butene oxide, 3,4-epoxy-1-butene, styrene oxide, and so on. Also, in our work on functionalization of PS$^-$Li$^+$ with 1-ethoxyethyl glycidyl ether (EEGE), [43] the capping reaction was again realized with a quantitative efficiency. All these references had given the result that capping reaction between living species and oxirane ring was rather efficient, quantitative and almost no any side reactions were accompanied, which were mainly due to the high aggregation degree of lithium alkoxides and their disability to initiate the further polymerization of oxirane ring. In this work, because of the inertness of allyl group, the living species would just attack the oxirane ring on AGE, and a new hydroxyl group was simultaneously generated (Scheme 2). Once the AGE agent was added into the red system of $^+$Li-PS$^-$Li$^+$ solution, one could observe that the color of system was changed into light yellow immediately, which meant that the alkoxides (-O$^-$Li$^+$) was actually formed. In order to ensure the

high efficiency of end-capping reaction, excess AGE agent (nine-fold) was fed. The successful LAP of St monomers was evidenced by the monomodal peak and symmetrical GPC curve with a narrow molecular weight distribution (PDI=1.10) (Fig. 1). Also, the ^{1}H NMR (Fig. 2A) and ^{13}C NMR (Fig. 3A) spectra of the synthesized AGE-PS-AGE were monitored. In Fig. 2A, except for the characteristic resonance signals of aromatic protons (-$C_6\boldsymbol{H}_5$-) on PS chain ascribed at 6.28-7.22 ppm, the resonance signal appeared at 5.16 ppm ($C\boldsymbol{H}_2$=CH-) and 5.78 ppm (CH_2=$C\boldsymbol{H}$-) confirmed the successful introduction of allyl group onto PS. Also, the signals ascribed to methane and methylene protons (-$C\boldsymbol{H}$(OH)$C\boldsymbol{H}_2$O$C\boldsymbol{H}_2$CH=CH_2) were observed at 3.50-4.00 ppm. In Fig 3A, the characteristic resonance signals of carbon atoms (-$\boldsymbol{C}_6H_5$-) were ascribed at 124-130 ppm, and the characteristic resonance signals of carbon atoms ($\boldsymbol{C}H_2$=CH-) and (CH_2=$\boldsymbol{C}$H-) were ascribed at 117ppm and 134ppm, respectively. Thus, the NMR results had actually proved the smooth coupling reaction of AGE agent with living $^+$Li-PS$^-$Li$^+$ species and the successful introduction of allyl group onto PS. Furthermore, the functionalized AGE-PS-AGE with defined structure was again well analyzed by MALDI-TOF MS (Fig. 4). As shown in Fig. 4A, a series of mono-peaks was observed for AGE-PS-AGE. When the mass spectrum was expanded (Fig. 4A'), the peak at m/z=6994.2 (a monoisoptic mass peak) was attributed to the functionalized AGE-PS-AGE [$C_6H_{10}O_2$-$(C_8H_8)_{64}$-$C_6H_{10}O_2$.Ag^+=6994.2, cal. 6994.39], and the m/z spacing of 104.1 between adjacent peaks was the mass of St monomeric unit. The absence of any minor peak series confirmed that the capping reaction at both $^+$Li-PS$^-$Li$^+$ end was rather successful and a high efficiency was actually achieved. According to the integral areas at 5.16 ppm ($C\boldsymbol{H}_2$=CH-), 5.78ppm (CH_2=$C\boldsymbol{H}$-), 6.28-7.22 ppm and the absolute molecular weight of AGE-PS-AGE obtained by MALDI-TOF MS, the capping efficiency of AGE agent to $^+$Li-PS$^-$Li$^+$ was calculated as 98.5%.

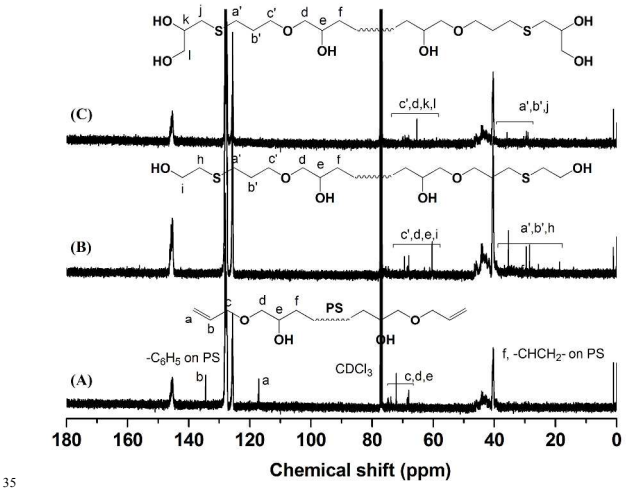

Fig. 3 ^{13}C NMR spectra of (A) AGE-PS-AGE, (B) ME-PS-ME and (C) MP-PS-MP (in $CDCl_3$).

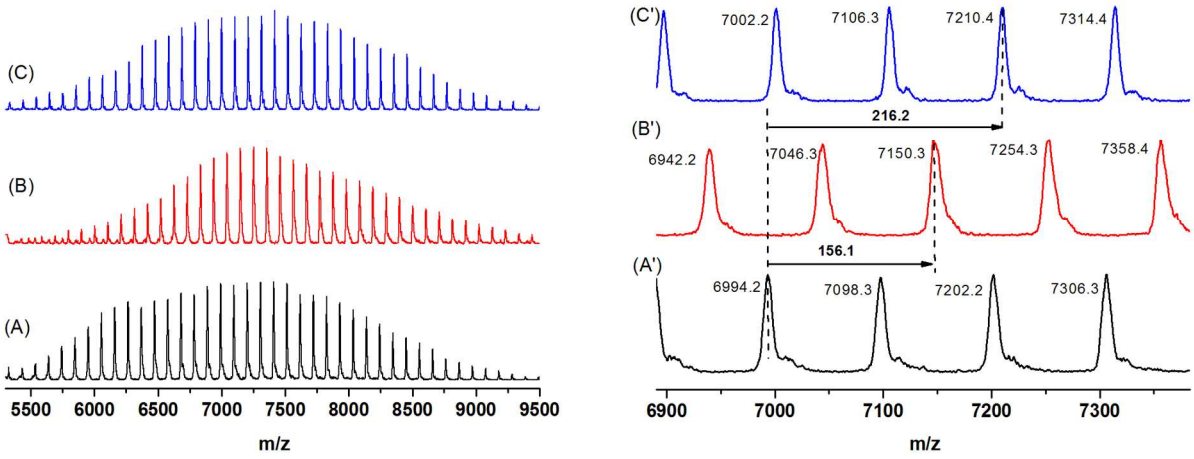

Fig. 4 The MALDI-TOF MS of (A and A') AGE-PS-AGE ($M_{n,GPC}$=7,500 g/mol), (B and B') ME-PS-ME and (C and C') MP-PS-MP.

Subsequently, by efficient thiol-ene addition reaction, one allyl group could be transferred into one or two hydroxyl groups. Using DMF as solvent and AIBN as catalyst, the ME-PS-ME with two hydroxyl groups at each end was obtained by reaction between 2-mercaptoethanol and the above AGE-PS-AGE (Scheme 3). From the ^{1}H NMR spectrum of ME-PS-ME (Fig. 2B), the disappearance of resonance signal at 5.16 ppm ($C\boldsymbol{H}_2$=CH-) and 5.78 ppm (CH_2=$C\boldsymbol{H}$-) confirmed that the allyl groups had been completely consumed. Also, the appearance of signals at 2.54 ppm and 2.69 ppm assigned to the methylene protons connected to sulfur atom (-$C\boldsymbol{H}_2$-S-$C\boldsymbol{H}_2$-) further confirmed the successful introduction of 2-mercaptoethanol. Similarly, the MP-PS-MP was obtained by thiol-ene addition reaction between AGE-PS-AGE and 3-mercapto-1,2-propanediol. The complete disappearance of resonance signals at 5.16 ppm and 5.78 ppm assigned to allyl group confirmed that almost 100 % efficiency of thiol-ene addition reaction was realized. From ^{13}C NMR spectra of ME-PS-ME (Fig. 3B) and MP-PS-MP (Fig. 3C), the complete disappearance of characteristic signals ascribed to carbon atoms at 117 ppm ($\boldsymbol{C}H_2$=CH-) and 134 ppm (CH_2=$\boldsymbol{C}$H-) and the new occurrence of signals ascribed to the carbon atoms on ME or MP groups also gave the same information that the allyl groups at PS end had been completely transformed into the

corresponding target groups. Again, the efficient transformation from AGE-PS-AGE to ME-PS-ME and MP-PS-MP was confirmed by MALDI-TOF MS measurement (Fig. 4). As shown in Fig. 4, an increase of 156.1 m/z from peak [$C_6H_{10}O_2$-$(C_8H_8)_{64}$-$C_6H_{10}O_2$.Ag^+=6994.2, cal. 6994.39] to peak [C_2H_6OS-$C_6H_{10}O_2$-$(C_8H_8)_{64}$-$C_6H_{10}O_2$-C_2H_6OS.Ag^+=7150.3] was attributed to the mass of introduced two 2-mercaptoethanol units. And the increase of 216.2 m/z from peak [$C_6H_{10}O_2$-$(C_8H_8)_{64}$-$C_6H_{10}O_2$.Ag^+=6994.2, cal. 6994.39] to peak [$C_3H_8O_2S$-$C_6H_{10}O_2$-$(C_8H_8)_{64}$-$C_6H_{10}O_2$- $C_3H_8O_2S$.Ag^+=7210.4] was attributed to the mass of introduced two 3-mercapto-1,2-propanediol units. Thus, the perfect coincident results from MALDI-TOF MS and NMR gave the information that the macro-initiators of ME-PS-ME and MP-PS-MP were actually and successfully synthesized.

Table 1 Data for dumbbell-shaped copolymers of PEO_x-*b*-PS-*b*-PEO_x and their precursors.

Entry	Samples	$M_{n,GPC}$[a] (g/mol)	PDI[a]	$M_{n,NMR}$[b] (g/mol)	DP_{PS}[c]	DP_{PEO}[d]	Percentage of PEO segment (%)[e]
	AGE-PS-AGE	3,700	1.14	2,500[f]	23		
1	PEO-PS-PEO	11,500	1.11	11,000	23	193	78.02
2	PEO_2-PS-PEO_2	7,700	1.16	10,400	23	180	76.80
3	PEO_3-PS-PEO_3	7,600	1.10	9,100	23	150	73.40
4	PEO_3-PS-PEO_3	7,400	1.13	8,100	23	127	68.99
5	PEO_3-PS-PEO_3	7,000	1.09	6,000	23	80	59.54
	AGE-PS-AGE	7,900	1.14	7,500[f]	71		
6	PEO-PS-PEO	14,700	1.17	22,000	71	330	66.29
7	PEO-PS-PEO	9,100	1.09	13,300	71	132	44.03
8	PEO_2-PS-PEO_2	7,900	1.11	9,400	71	43	20.40
9	PEO_3-PS-PEO_3	9,800	1.14	11,700	71	95	36.15

[a] Determined by GPC with THF as solvent using PS standards. [b] The molecular weights of copolymers were calculated according to ^{1}H NMR using Formula 1. [c] The degree of polymerization (DP_{PS}) was calculated according to the Formula: $DP_{PS} = M_{n,MALDI-TOF\ MS,PS}/104$. [d] The degree of polymerization (DP_{PEO}) was calculated according to the Formula: $DP_{PEO} = (M_{n,NMR,(PEOx-b-PS-b-PEOx)} - M_{n,MALDI-TOF\ MS,PS})/44$. [e] The percentage of PEO segment (%) was calculated according to the Formula: $\%_{PEO} = D_{PEO}x44/M_{n,NMR,(PEOx-b-PS-b-PEOx)}$. [f] Determined by MALDI-TOF MS measurement.

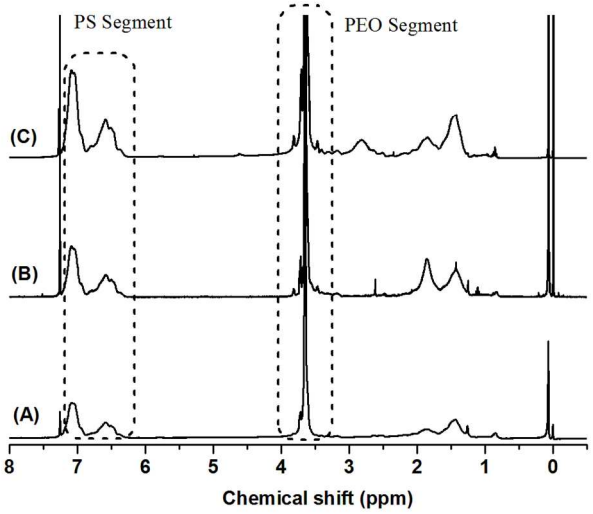

Fig. 5 ^{1}H NMR spectra of PEO_3-*b*-PS-*b*-PEO_3 with the same PS segment but different length of PEO segments: (A) Entry 3, (B) Entry 4, and (C) Entry 5 (in $CDCl_3$).

Finally, the target copolymers PEO_x-*b*-PS-*b*-PEO_x were obtained by ROP of EO monomers using the above AGE-PS-AGE, ME-PS-ME and MP-PS-MP as macro-initiators and DPMK as deprotonation agent, respectively (Scheme 3). Typically, because of the rapid exchange ratio (which was faster than the propagation ratio) between living species -O^-K^+ and the dormant -OH, the ROP mechanism was endowed with the living character. According to the references, [44] the primary and secondary hydroxyl could give the uniform growth of PEO chains under certain polymerization conditions. Using the similar polymerization system in this contribution, all the hydroxyl groups would have the ability to initiate the polymerization of EO monomers, and the designed architecture of PEO_x-*b*-PS-*b*-PEO_x with defined numbers of arms could be actually obtained. From Fig. 1, it could be observed that the GPC traces of obtained PEO-*b*-PS-*b*-PEO, PEO_2-*b*-PS-*b*-PEO_2 and PEO_3-*b*-PS-*b*-PEO_3 were all given with monomodal peaks and low PDIs, which also gave the conclusion that the ROP mechanism was smoothly proceeded. However, an asymmetrical GPC trace with a tail at longer elution time were always detected due to the strong adsorption of PEO segment with the column in THF solvent (which was not a good solvent for PEO segment) rather than the existence of PS homopolymers, and the similar phenomenon was also reported in our previous work[43] and other's works. [45] In order to further confirm this consumption, the copolymers were verified by the TLC method using THF as developing agent. The absence of any PS signal in the front edge under 254nm UV detector confirmed that there was actually not any PS homopolymer existed in copolymers. The composition of copolymers were further traced by ^{1}H MNR spectrum. In order to avoid the formation of micelles in a selective solvent,[2a,45] the ^{1}H NMR measurement of copolymers was carried out in $CDCl_3$ solvent, which was a good solvent for both PEO and PS segments. [46] As shown in Fig. 5, the characteristic resonance signal of aromatic protons (-$C_6\boldsymbol{H}_5$-) on PS segment at 6.28-7.22 ppm and that of methylene protons (−C$\boldsymbol{H}_2$C$\boldsymbol{H}_2$O−) on PEO segment at 3.05-3.70 ppm were all well discriminated. On the other hand, the molecular weight of PEO_x-*b*-PS-*b*-PEO_x determined by GPC measurement using THF as eluent was unreliable because THF was not a good solvent for PEO segment and the PEO_x-*b*-PS-*b*-PEO_x might aggregated into

micellar structures by self-association in THF, and this phenomenon was also reported in references[2a,47] and our previous work.[43] Alternatively, according to above ^{1}H MNR spectrum and the already known absolute molecular weight of AGE-PS-AGE precursor, the accurate molecular weight of copolymers could be derived from Formula:

$$M_{n,NMR} = \frac{A_{PEO}/4}{A_{PS}/5} \times \frac{M_{n,MALDI-TOF\ MS,PS}}{104} \times 44 + M_{n,MALDI-TOF\ MS,PS} + 2 \times R \qquad (1)$$

Here, the A_{PEO} and A_{PS} represented the integral areas of resonance signals of aromatic protons (-$C_6\boldsymbol{H}_5$-) at 6.28-7.22 ppm and that of methylene protons (−C$\boldsymbol{H}_2$C$\boldsymbol{H}_2$O−) at 3.05-3.70 ppm, respectively. $M_{n,MALDI\text{-}TOF\ MS,PS}$ was the absolute molecular weight of AGE-PS-AGE precursor obtained from MALDI-TOF MS measurement. The value of 104 and 44 were the molecular weight of St and EO monomeric unit, respectively. The letter R was equal to 0 (for PEO-*b*-PS-*b*-PEO), 78 (for PEO_2-*b*-PS-*b*-PEO_2) or 108 (for PEO_3-*b*-PS-*b*-PEO_3), and the values of 78 and 108 were corresponded to the molecular weight of introduced ME and MP residues, respectively.

Interestingly, comparing the molecular weight of the copolymers obtained from GPC with that from NMR measurement, one could also discriminated that the apparent molecular weights from GPC measurement have less linear dependence with their absolute molecular weights from NMR measurement. For example, the PEO-*b*-PS-*b*-PEO in Entry 1 and PEO_2-*b*-PS-*b*-PEO_2 in Entry 2 had a difference of 600 g/mol in their absolute molecular weights from NMR measurement, however, there was a difference of 3,800 g/mol from their GPC measurement. Alternatively, the samples in Entry 2, Entry 3, Entry 4 and Entry 5 had the very close apparent molecular weights from GPC measurement, however, there were much differences between their absolute molecular weights. These phenomena could be attributed to the varied length of PEO segment and the increasing branching of copolymers from PEO-*b*-PS-*b*-PEO, PEO_2-*b*-PS-*b*-PEO_2 to PEO_3-*b*-PS-*b*-PEO_3. Also, these phenomena might give the information that the topologies of copolymers actually induced some special properties of copolymers, and herein, the crystallization behavior of these synthesized copolymers will be discussed in the following section.

The Crystallization Behavior Copolymers of PEO_x-*b*-PS-*b*-PEO_x

Typically, the PS was an amorphous segment, while the PEO was a crystalline segment.[48] As shown in Table 1, the PS and PEO segments with different length were designed and synthesized by the versatile LAP and ROP mechanisms. As an important target, the crystallization behavior of these synthesized copolymers was investigated and compared in this contribution.

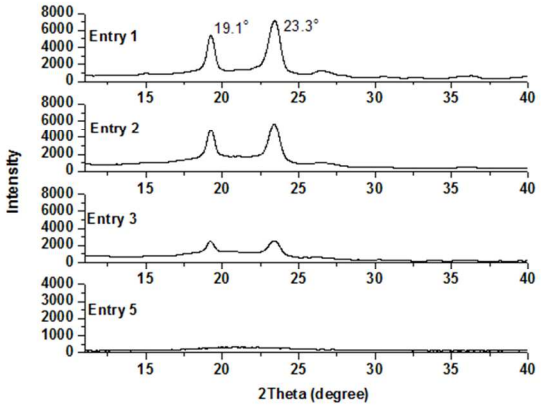

Fig. 6 X-ray diffraction patterns for PEO-*b*-PS-*b*-PEO (Entry 1), PEO_2-*b*-PS-*b*-PEO_2 (Entry 2) and PEO_3-*b*-PS-*b*-PEO_3 (Entry 3 and Entry 5).

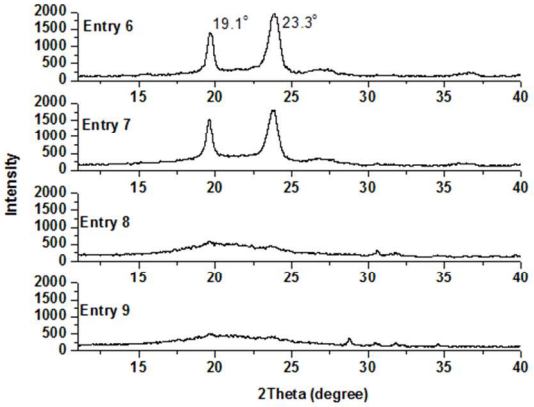

Fig. 7 X-ray diffraction patterns for PEO-*b*-PS-*b*-PEO (Entry 6 and Entry 7), PEO_2-*b*-PS-*b*-PEO_2 (Entry 8) and PEO_3-*b*-PS-*b*-PEO_3 (Entry 9).

By XRD measurement, the crystallization behavior of PEO_x-*b*-PS-*b*-PEO_x was firstly studied. All the samples were measured at room temperature without annealing. Typically, the linear PEO showed two intensive diffraction peaks at 19.1° and 23.3°, respectively.[49] As shown in Fig. 6, with the close percentage of PEO segment but varied numbers of side PEO arms, the intensity of diffraction peak of PEO crystallite decreased from the copolymers of PEO-*b*-PS-*b*-PEO (Entry 1) to PEO_2-*b*-PS-*b*-PEO_2 (Entry 2) and PEO_3-*b*-PS-*b*-PEO_3 (Entry 3). For these three samples with the close percentage of PEO segment, the length of PEO arms were shortened with the increase of numbers of side arms, and correspondingly, the shorter PEO segment and the increased terminal PEO end would severely interrupted the crystallization ability of copolymers.

Alternatively, when the numbers of PEO arms were fixed but their percentages were varied, the crystallization behavior of copolymers would lead to another result. Comparing the XRD traces for Entry 3 with that for Entry 5, no any diffraction signals could be observed in XRD trace for the latter when PEO content was merely decreased to 59.54 %. However, comparing the XRD traces for Entry 6 with that for Entry 7, the strong signals could

still be discriminated at 19.1° and 23.3° even though the PEO content was decreased to 44.03 % for Entry 7(Fig. 7). These results preliminarily gave the conclusion that the degree of branching would exert more effect on the crystallization behavior than the percentage of PEO segment did.

Furthermore, the crystallization behavior of copolymers was verified by DSC measurement. The crystallization temperature (T_c) was obtained from the cooling run, and the melting temperature (T_m) was obtained from the second heating run. Usually, for the linear PEO homopolymer with the molecular weight about M_n= 5000 g/mol, the T_m and T_c were observed at 63.9 °C and 43.9 °C, respectively.[50] As shown in Fig. 8, for the sample of PEO-*b*-PS-*b*-PEO (Entry 1), the single T_c and T_m were clearly discriminated at 32.9 °C and 53.6 °C, respectively, which were all lower than those of PEO homopolymer. However, for the sample of PEO_2-*b*-PS-*b*-PEO_2 (Entry 2), which has close percentage of PEO segment but different numbers of side PEO arms to the sample in Entry 1, except for a decreased T_m peak ascribed at 31.3 °C and a T_c peak ascribed at -21.0 °C were observed in the heating curve, there was almost not any T_c detected in the cooling run. We concluded that, because of the increased complexity of the architectures of PEO_2-*b*-PS-*b*-PEO_2 in Entry 2, the PEO segment could not be arranged into the crystalline in the cooling program, and the insufficient crystallization of PEO segment was maintained in the sample. Alternatively, in the following heating program, some of PEO segment in amorphous phase might again be folded into the crystalline under certain temperature by thermal crystallization procedure. This phenomenon had also been reported by reference.[51] Similarly, the sample of PEO_3-*b*-PS-*b*-PEO_3 (Entry 3) also gave a T_c at -32.5 °C corresponded to thermal crystallization and a typical T_m at 32.3 °C in the heating curve, and there was also not any T_c could be observed in the cooling curve.

Again, for the samples with the same numbers of PEO arms but varied percentage of PEO segment, the DSC results of the PEO_3-*b*-PS-*b*-PEO_3 series would also give a different tendency to that of PEO-*b*-PS-*b*-PEO series. For example, comparing the DSC curve for Entry 3 with that for Entry 5 (Fig 8), no any peaks could be discriminated in DSC curve for the latter Entry 5 because of the decreased percentage of PEO segment (59.54 %). However, comparing the DSC curves for Entry 6 with that for Entry 7 (Fig 9), both samples gave the DSC curves with defined T_m and T_c peaks (even though the percentage of PEO segment in latter Entry 7 was decreased to 44.03 %) because of the linear architecture of PEO-*b*-PS-*b*-PEO.

From Fig. 10 for DSC curves of Entry 8 and Entry 9, there was almost not obvious signal for the crystallization behavior (such as the T_m and T_c peaks) of samples, except that there was only a weak T_m peak at 38.5 °C, which were rather consistent with the results from their XRD measurement (Fig. 7). The reasons might be attributed to the largely lowered PEO content or increased number of side arms, as well as the increased length of PS segment. On the other hand, it was worth noting that even with the increased length of PS segment (7,500 g/mol) for samples in Entry 8 and Entry 9, no any trace of the glass transition temperature (T_g) for PS segment could be discriminated.

Thus, the DSC results again gave the information that the degree of branching would contribute greater effect on the crystallization behavior of copolymers than the percentage of individual segment did.

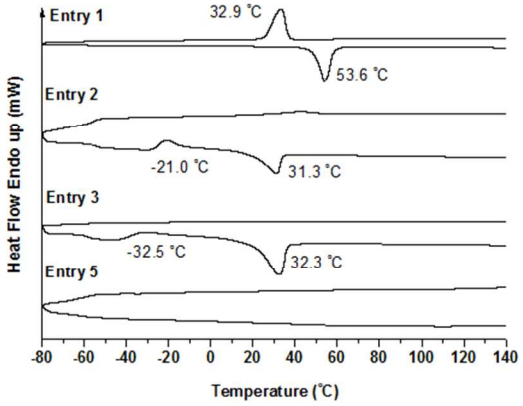

Fig. 8 DSC trace of copolymer PEO-*b*-PS-*b*-PEO (Entry 1), PEO_2-*b*-PS-*b*-PEO_2 (Entry 1) and PEO_3-*b*-PS-*b*-PEO_3 (Entry 3 and Entry 5).

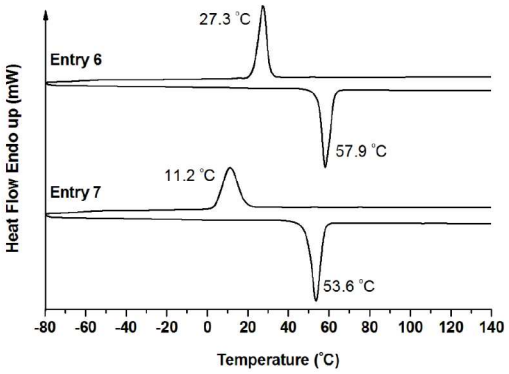

Fig. 9 DSC trace of copolymer PEO-*b*-PS-*b*-PEO (Entry 6 and Entry 7).

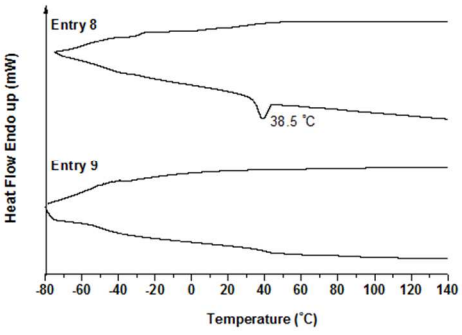

Fig. 10 DSC trace of copolymer PEO_2-*b*-PS-*b*-PEO_2 (Entry 8) and PEO_3-*b*-PS-*b*-PEO_3 (Entry 9).

Finally, the crystallization behavior was also investigated by POM measurement (Fig. 11). From the POM micrograph of PEO-*b*-PS-*b*-PEO (Entry 1), we could clearly observe that the big

spherulites of PEO segment could be formed in 30 minutes. With the increase of the numbers of PEO arms, the crystallization behavior was significantly affected. Obviously, from the sample of PEO-*b*-PS-*b*-PEO (Entry 1) to PEO_2-*b*-PS-*b*-PEO_2 (Entry 2) and PEO_3-*b*-PS-*b*-PEO_3 (Entry 3), the longer crystallization time was needed and only smaller spherulites could be observed.

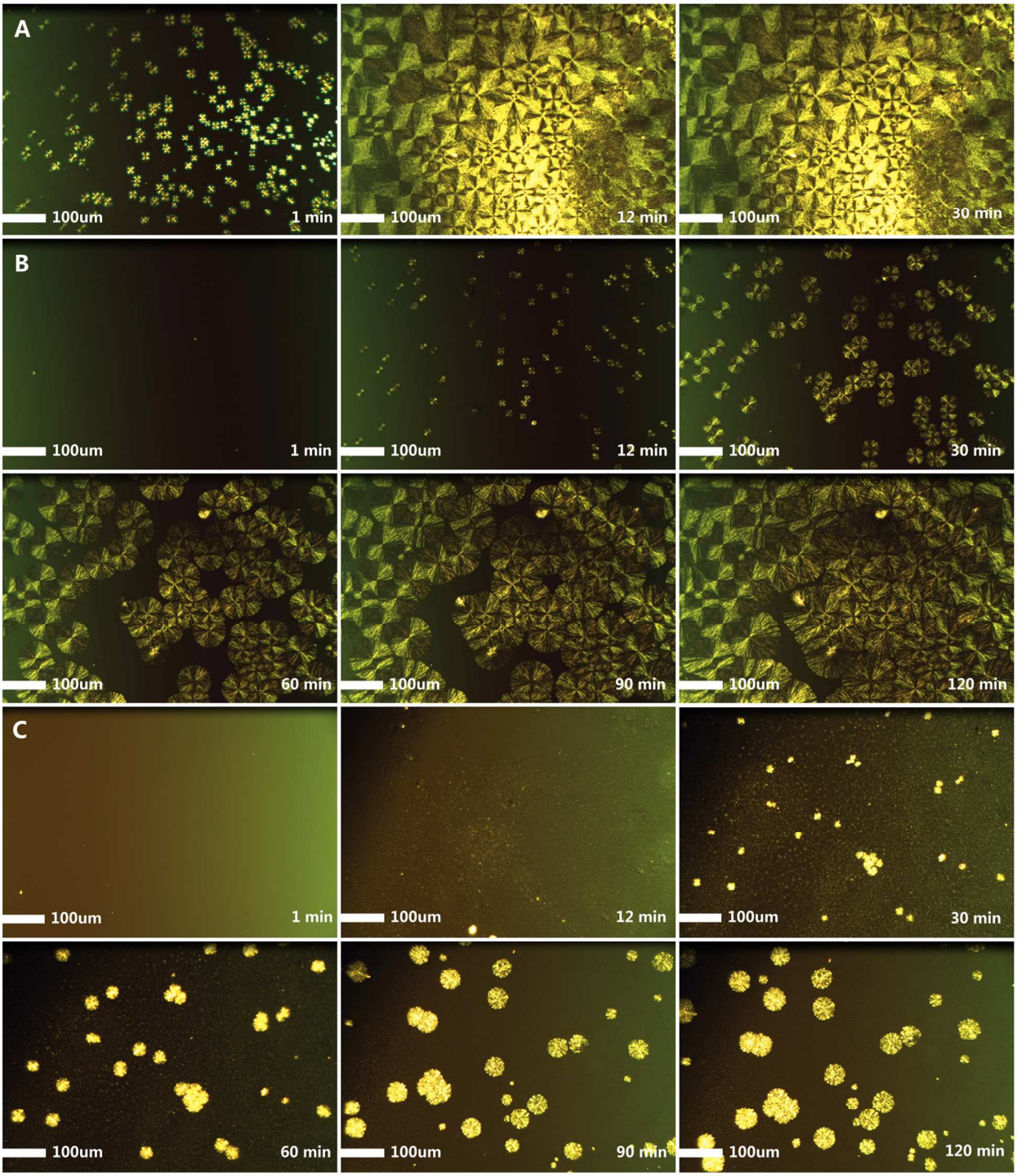

Fig. 11 Optical microscopy images of copolymers (scale bar = 100um): (A) PEO-*b*-PS-*b*-PEO (Entry 1), (B) PEO_2-*b*-PS-*b*-PEO_2 (Entry 2), and (C) PEO_3-*b*-PS-*b*-PEO_3 (Entry 3).

Thus, all the above results indicated that the degree of branching and compositions actually exerted some important effects on the crystallization behaviors of synthesized dumbbell-shaped copolymers PEO_x-*b*-PS-*b*-PEO_x. The existence of PS segment largely interrupted the crystallization behavior of PEO segment, and the existence of crystalline PEO segment largely restricted the mobility of PS segment and affected its T_g. Comprehensively, the degree of branching derived from various complicated topologies might gave the primary contribution to the crystallization behavior.

CONCLUSIONS

Series of well-defined dumbbell-shaped copolymers PEO_x-*b*-PS-*b*-PEO_x (x=1, 2, 3) consisting of PEO and PS segments were successfully synthesized by LAP, ROP mechanism and the efficient thiol-ene addition reaction. This versatile synthetic route might be further explored to synthesize other copolymers with complicated architectures. Also, crystallization behavior of the copolymers with close compositions but different topologies, or conversely, with different compositions but the same topologies, were investigated and compared. The preliminary results confirmed that the topologies of copolymers actually have primary contribution to the crystallization behavior.

Acknowledgements

We appreciate the financial support of this research by the Natural Science Foundation of China (21274024).

Notes and references

State Key Laboratory of Molecular Engineering of Polymers, Department of Macromolecular Science, Fudan University, Shanghai 200433, China. Fax: 86 21 6564 0293; Tel: 86 21 6564 3049; E-mail: gwwang@fudan.edu.cn

1 (a) A. Vazaios, D. J. Lohse and N. Hadjichristidis, *Macromolecules* 2005, **38**, 5468-5474. (b) L. Andruzzi, A. Hexemer, X. F. Li, C. K. Ober, E. J. Kramer, G. Galli, E. Chiellini and D. A. Fischer, *Langmuir* 2004, **20**, 10498-10506. (c) F. J. Xu, Y. Song, Z. P. Cheng, X. L. Zhu, C. X. Zhu, E. T. Kang and K. G. Neoh, *Macromolecules* 2005, **38**, 6254-6258. (d) V. Percec, T. Guliashvili, J. S. Ladislaw, A. Wistrand, A. Stjerndahl, M. J. Sienkowska, M. J. Monteiro and S. Sahoo, *J. Am. Chem. Soc.* 2006, **128**, 14156-14165. (e) H. F. Gao and K. Matyjaszewski, *J. Am. Chem. Soc.* 2007, **129**, 6633-6639. (f) W. H. Binder and R. Sachsenhofer, *Macromol. Rapid. Commun*. 2007, **28**, 15-54.

2 (a) H. Zhang and E. Ruckenstein, *Macromolecules* 2000, **33**, 814-819. (b) K. Se, H. Yamazaki, T. Shibamoto, A. Takano and T. Fujimoto, *Macromolecules* 1997, **30**, 1570-1576.

3 M. Gauthier, L. Tichagwa, J. S. Downey and S. Gao, *Macromolecules* 1996, **29**, 519-527.

4 C. Lee, H. Lee, W. Lee, T. Chang and J. Roovers, *Macromolecules* 2000, **33**, 8119-8121.

5 J. Teng and E. R. Zubarev, *J. Am. Chem. Soc.* 2003, **125**, 11840-11841.

6 N. Hadjichristidis, M. Pitsikalis, S. Pispas and H. Iatrou, *Chem. Rev.* 2001, **101**, 3747-3792.

7 Y. Yagci and M. A. Tasdelen, *Prog. Polym. Sci.* 2006, **31**, 1133-1170.

8 S. E. Stiriba, H. Kautz and H. Frey, *J. Am. Chem. Soc.* 2002, **124,** 9698-9699.

9 R. Djalali, S. Y. Li and M. Schmidt, *Macromolecules* 2002, **35**, 4282-4288.

10 M. Zhang, M. Drechsler and A. H. E. Muller, *Chem. Mater.* 2004, **16**, 537-543.

11 L. H. He, J. Huang, Y. M. Chen, X. J. Xu and L. P. Liu, *Macromolecules* 2005, **38**, 3845-3851.

12 L. Huang, H. Yuan, D. B. Zhang, Z. Zhang, J. Guo and J. M. Ma, *Appl. Surf. Sci*. 2004, **225**, 39-46.

13 L. M. Wu and Q. C. Zou, *J. Polym. Sci. Polym. Phys.* 2007, **45**, 2015-2022.

14 (a) Y. Gao and H. L. Liu, *J. Appl. Polym. Sci*. 2007, **106**, 2718-2723. (b) C. Y. Luo, X. Han, Y. Gao, H. L. Liu and Y. Hu, *J. Macromol. Scit. B*. 2010, **49**, 440-453.

15 (a) S. Y. Cheng, Z. S. Xu and J. Yuan, *J. Acta. Chim. Sinica.* 2000, **58**, 368-370. (b) R. Francis, D. Taton, J. L. Logan, P. Masse, Y. Gnanou and R. S. Duran, *Macromolecules* 2003, **36**, 8253-8259.

16 (a) T. Kimura and Y. Yamauchi, *Langmuir* 2012, **28**, 12901-12908. (b) D. Chandra, M. Bekki, M. Nakamura, S. Sonezaki, T. Ohji, K. Kato and T. Kimura, *J. Mater. Chem*. 2011, **21**, 5738-5744.

17 (a) Y. J. Cheng, M. Wolkenhauer, G. G. Bumbu and J. S. Gutmann, *Macromol. Rapid. Comm.* 2012, **33**, 218-224. (b) T. Ghoshal, M. T. Shaw, C. T. Bolger, J. D. Holmes and M. A. Morris, *J. Mater. Chem*. 2012, **22**, 12083-12089.

18 (a) N. V. Salim, T. L. Hanley, L. Waddington, P. G. Hartley and Q. P. Guo, *Macromol. Rapid. Comm*. 2012, **33**, 401-406. (b) Y. Zhang, H. Li, Y. Q. Liu and J. Wang, *Chem. Commun.* 2012, **48**, 8538-8540.

19 (a) B. M. Rosen, G. Lligadas, C. Hahn and V. Percec, *J. Polym. Sci. Part A: Polym. Chem.* 2009, **47**, 3931-3939. (b) B. M. Rosen, G. Lligadas, C. Hahn and V. Percec, *J. Polym. Sci. Part A: Polym. Chem.* 2009, **47**, 3940-3948.

20 (a) J. W. Chan, C. E. Hoyle and A. B. Lowe, *J. Am. Chem. Soc.* 2009, **131**, 5751-5753. (b) V. T. Huynh, G. J. Chen, P. D. Souza and M. H. Stenzel, *Biomacromolecules* 2011, **12**, 1738-1751. (c) B. Yu, J. W. Chan, C. E. Hoyle and A. B. Lowe, *J. Polym. Sci. Part A: Polym. Chem.* 2009, **47**, 3544-3557.

21 (a) A. Dondoni, *Angew. Chem. Int. Ed.* 2008, **47**, 8995-8997. (b) C. E. Hoyle and C. N. Bowman, *Angew. Chem. Int. Ed.* 2010, **49**, 1540-1573.

22 T. Sarbu, K. Y. Lin, J. Ell, D. J. Siegwart, J. Spanswick and K. Matyjaszewski, *Macromolecules* 2004, **37**, 3120-3127.

23 P. Siemsen, R. C. Livingston and F. Diederich, *Angew. Chem. Int. Ed.* 2000, **39**, 2632-2657.

24 (a) R. Kandre, K. Feldman, H. E. H. Meijer, P. Smith and A. D. Schluter, *Angew. Chem. Int. Ed.* 2007, **46**, 4956-4959. (b) W. G. Huang, L. J. Su and Z. J. Bo, *J. Am. Chem. Soc.* 2009, **131**, 10348-10349.

25 (a) E. C. Hagberg, M. Malkoch, Y. Ling, C. J. Hawker and K. R. Carter, *Nano. Lett.* 2007, **7**, 233-237. (b) V. S. Khire, A. W. Harant, A. W. Watkins, K. S. Anseth and C. N. Bowman, *Macromolecules* 2006, **39**, 5081-5086.

26 (a) A. W. Harant, V. S. Khire, M. S. Thibodaux and C. N. Bowman, *Macromolecules* 2006, **39**, 1461-1466. (b) V. S. Khire, T. Y. Lee and C. N. Bowman, *Macromolecules* 2008, **41**, 7440-7447. (c) L. A. Connal, C. R. Kinnane, A. N. Zelikin and F. Caruso, *Chem. Mater.* 2009, **21**, 576-578.

27 (a) V. S. Khire, D. S. W. Benott, K. S. Anseth and C. N. Bowman, *J. Polym. Sci. Part A: Polym. Chem.* 2006, **44**, 7027-

7039. (b) A. E. Rydholma, C. N. Bowmana and K. S. Anseth, *Biomaterials* 2005, **26**, 4495-4506. (c) A.Dondoni, *Angew. Chem. Int. Ed.* 2008, **47**, 8995-8997.

28 M. Sangermano, R. Bongiovanni, G. Malucelli, A. Priola, A. Harden and N. Rehnber, *J. Polym. Sci. Part A: Polym. Chem.* 2002, **40**, 2583-2590.

29 (a) H. Y. Wei, A. F. Senyurt, S. Jonsson and, C. E. Hoyle, *J. Polym. Sci. Part A: Polym. Chem.* 2007, **45**, 822-829. (b) J. Shin, S. Nazarenko and C. E. Hoyle, *Macromolecules* 2008, **41**, 6741-6746. (c) L. Kwisnek, S. Nazarenko and C. E. Hoyle, *Macromolecules* 2009, **42**, 7031-7041.

30 K. L. Killops, L. M. Campos and C. J. Hawker, *J. Am. Chem. Soc.* 2008, **130**, 5062-5064.

31 C. Rissing and D. Y. Son, *Organometallics* 2009, **28**, 3167–3172.

32 C. Nilsson, N. Simpson, M. Malkoch, M. Johansson and E. Malmstro, *J. Polym. Sci. Part A: Polym. Chem.* 2008, **46**, 1339-1348.

33 L. M. Campos, K. L. Killops, R. Sakai, J. M. J. Paulusse, D. Damiron, E. Drockenmuller, B. W. Messmore and C. J. Hawker, *Macromolecules* 2008, **41**, 7063-7070.

34 R. L. A. David and J. A. Kornfield, *Macromolecules* 2008, **41**, 1151-1161.

35 A. Gress, A. Volkel and H. Schlaad, *Macromolecules* 2007, **40**, 7928-7933.

36 J. S. Parent and S. S. Sengupta, *Macromolecules* 2005, **38**, 5538-5544.

37 M. Li, P. De, S. R. Gondi and B. S. Sumerlin, *J. Polym. Sci. Part A: Polym. Chem.* 2008, **46**, 5093-5100.

38 Z. P. Tolstyka, J. T. Kopping and H. D. Maynard, *Macromolecules* 2008, **41**, 599-606.

39 (a) S. Peleshanko, J. Jeong, R. Gunawidjaja and V. V. Tsukruk, *Macromolecules* 2004, **37**, 6511-6522. (b) U. S. Jeng, Y. S. Sun, H. Y. Lee, C. H. Hsu and K. S. Liang, *Macromolecules* 2004, **37**, 4617-4622.

40 B. Lotz and A. Kovacs, *J. Polym. Prepr. Am. Chem. Soc. Polym. Chem. Div.* 1969, ***10***, 820.

41 Y. N. Zhang, G. W. Wang and J. L. Huang, *Macromolecules* 2010, **4**,10343-10347.

42 (a) R. P. Quirk, Q. Ge, M. A. Arnould and C. Wesdemiotis, *Macromol. Chem. Phys.* 2001, **202**, 1761-1767. (b) R. P. Quirk and G. M. Lizarraga, *Macromolecules* 1998, **31**, 3424-3430. (c) R. P. Quirk, H. Hasgawa, D. L. Gomochak, C. Wesdemiotis and K. Wollyung, *Macromolecules* 2004, **37**, 7146-7155. (d) R. P. Quirk and W. C. Chen, *Macromol. Chem.* 1982, **183**, 2071-2076. (e) R. P. Quirk, D. L. Gomochak, C. Wesdemiotis and M. A. Arnold, *J. Polym. Sci. Part A: Polym. Chem.* 2003, **41**, 947-957. (f) R. P. Quirk and J. J. Ma, *J. Polym. Sci. Part A: Polym. Chem.* 1988, **26**, 2031-2037. (g) R. P. Quirk, D. L. Pickel and H. Hasegawa, *Macromol. Symp.* 2005, **226**, 69-77.

43 (a) G. W. Wang and J. L. Huang. *J. Polym. Sci. Part A: Polym. Chem.* 2008, **46**, 1136-1150. (b) G. W. Wang and J. L. Huang. *Macromol. Rapid Commun.* 2007, **28**, 298-304.

44 (a) X.S. Feng, D. Taton, E. L. Chaikof and Y. Gnanou. *J. Am. Chem. Soc.* 2005, **127**, 10956-10966. (b) X.S. Feng, D. Taton, E. L. Chaikof and Y. Gnanou. *Macromolecules* 2009, **42**, 7292–7298

45 (a) F. Calderara, Z. Hruska, G. Hurtrez, T. Nugay and G. Riess, *Makromol. Chem*. 1993, **194**, 1411-1420. (b) M. Teodorescu, M. Dimonie, C. Draghici and G. Vasilievici, *Polym. Int*. 2004, **53**, 1987-1993. (c) R. P. Quirk, J. Kim, C. Kausch and M. Chun, *Polym. Int.* 1996, **39**, 3-10.

46 (a) J. L. Hedrick, M. Trollsas, C. J. Hawker, B. Atthoff, H. Claesson, A. Heise, R. D. Miller, D. Mecerreyes, R. Jerome and P. Dubois, *Macromolecules* 1998, **31**, 8691-8705. (b) A. Heise, J. L. Hedrick, M. Trollsas, R. D. Miller and C. W. Frank, *Macromolecules* 1999, **32**, 231-234.

47 S. Angot, D. Taton and Y. Gnanou, *Macromolecules* 2000, **33**, 5418-5426.

48 (a) A. Boschetti-de-Fierro, A. J. Mueller and V. Abetz, *Macromolecules* 2007, **40**, 1290-1298. (b) N. Lin and A. Dufresne, *Macromolecules* 2013, **46**, 5570-5583. (c) C. He, J. Sun, T. Zhao, Z. Hong, X. Zhuang, X. Chen and X. Jing, *Biomacromolecules* 2006, **7**, 252-258. (d) C. He, J. Sun, J. Ma, X. Chen and X. Jing, *Biomacromolecules* 2006, **7**, 3482-3489.

49 G. Maglio, G. Nese, M. Nuzzo and R. Palumbo, *Macromol. Rapid. Commun.* 2004, **25**, 1139-1144.

50 C. Y. Liu, K. Lv, B. Huang, C. L. Hou and G. W. Wang, *RSC. Adv.* 2013, **3**, 17945-17953.

51 H. Yu, A. Natansohn, M. A. Singh and I. Torriani, *Macromolecules* 2001, **34**, 1258-1266.